Decentralized Control Schemes for Industrial Robot Manipulators

Lorenzo Sciavicco   Bruno Siciliano

Dipartimento di Informatica e Sistemistica
Università degli Studi di Napoli Federico II
Via Claudio 21, 80125 Napoli, Italy
Tel: +39 81 768-3179 — Fax: +39 81 768-3186
E-mail: siciliano@napoli.infn.it

Summary

The design of decentralized robust control schemes for industrial robot manipulators is the topic of this paper. The goal is to achieve good disturbance rejection and trajectory tracking capabilities in spite of dynamic coupling torques. Three schemes are presented that exploit joint position feedback, joint position + velocity feedback, joint position + velocity + acceleration feedback, respectively. The performance is improved by nesting more loops around the disturbance. Enhanced tracking is obtained by resorting to a linear feedforward action.

1. Introduction

Industrial robot manipulators are conventionally controlled by decentralized linear controllers at each independent joint. In fact, it is argued that, when robot joints have high gear ratios, the nonlinear coupling dynamic terms can be neglected since the actuator inertias reported at the joints dominate over the configuration-dependent terms. Moreover, industrial robot operational speeds are usually quite low, and therefore Coriolis/centrifugal terms are also not compensated.

It is known that, in the case of direct-drive manipulators, the dynamic terms play a significant role for high-speed motions [1]. A large number of model-based control schemes were proposed [2,3], including adaptive control algorithms [4,5,6]. More recently, however, it was demonstrated that also for industrial robot manipulators with high gear ratios dynamic compensation yields significant reduction of tracking errors [7,8].

The present work is based on the preliminary results in [9] and proposes new different control schemes of decentralized type which are shown to guarantee satisfactory tracking capabilities in spite of inertia and load variations. Three different schemes are proposed: position feedback, position + velocity feedback, position + velocity + acceleration feedback. The basic idea is to adopt a PI action for the inmost feedback loop, so as to get perfect steady-state disturbance torque rejection. It is shown that the third scheme achieves the best performance in terms of disturbance rejection ratio and recovery time during the transients. The problem of lack of direct acceleration measurements is solved by using a state variable filter to reconstruct them. Further, it is shown how linear feedforward compensation confers enhanced tracking capabilities to the schemes in case of good model accuracy.

2. Decentralized Control

It is well known that the dynamic model of a robot manipulator in free space is given by

$$B(q)\ddot{q} + C(q,\dot{q})\dot{q} + g(q) = \tau \tag{1}$$

where q is the $(n \times 1)$ vector of joint variables, B is the $(n \times n)$ positive definite symmetric inertia matrix, $C\dot{q}$ is the $(n \times 1)$ vector of Coriolis and centrifugal forces, g is the $(n \times 1)$ vector of gravitational forces, and τ is the $(n \times 1)$ vector of joint driving forces.

To control the motion of the manipulator means to determine the forces τ that allow the execution of a motion $q(t)$ such that it is

$$q(t) = q_d(t)$$

as closely as possible, where $q_d(t)$ indicates the vector of reference joint variables.

Focusing on the case of gear-driven robots, the joint forces are provided by the actuators via kinematic transmissions that perform a motion transformation from the
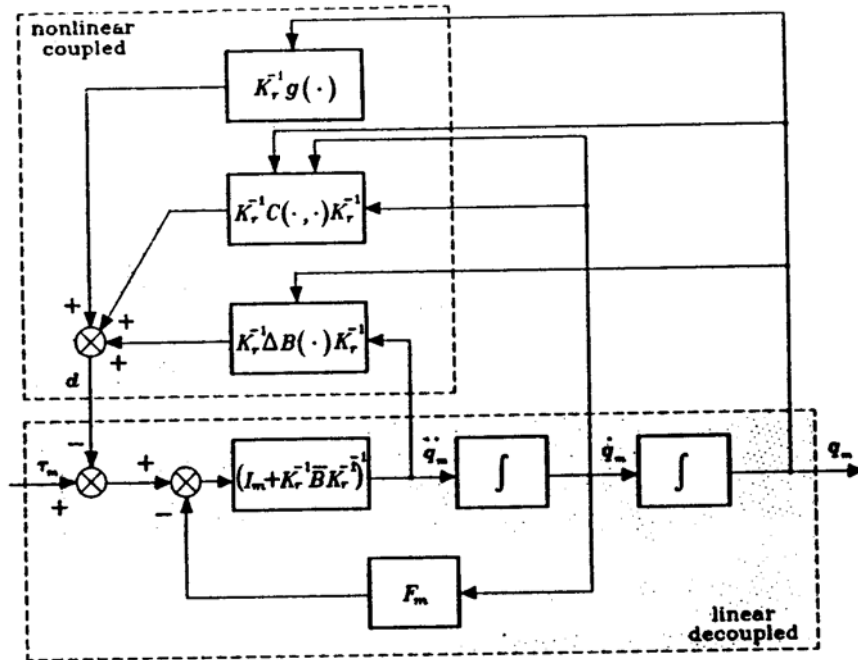

Figure 1 — Block diagram scheme of the dynamics of a gear-driven industrial robot manipulator.

motors to the links. If q_m is the $(n \times 1)$ vector of actuator displacements, the following relation is obtained

$$K_r q = q_m \tag{2}$$

where K_r is an $(n \times n)$ diagonal matrix whose elements are usually much greater than unity.

Due to the presence of gear reductions, the vector of actuator driving forces τ_m is given by

$$\tau_m = I_m \ddot{q}_m + F_m \dot{q}_m + K_r^{-1}\tau \tag{3}$$

where I_m and F_m are diagonal matrices whose elements are the inertias and viscous friction coefficients of the gear reduction motors, and $K_r^{-1}\tau$ is the vector of required joint torques resulting at the actuator axes.

At this point, observing that the diagonal elements of $B(q)$ contain inertia moments that do not depend on the joint configuration and configuration-dependent terms of sinusoidal functions, the inertia matrix can be decomposed as
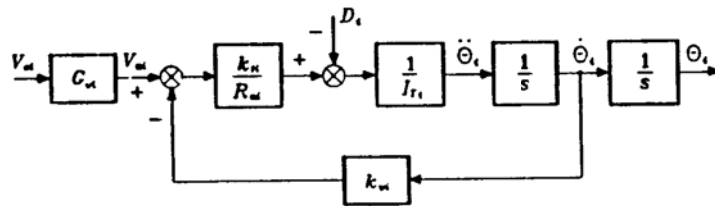
$$B(q) = \bar{B} + \Delta B(q) \tag{4}$$

Figure 2 — Block diagram scheme of the dynamics of an individual manipulator joint.

where $\bar{B}$ is a diagonal matrix whose constant elements represent the average values of joint inertias. Plugging (2–4) into (1) gives

$$\tau_m = (I_m + K_r^{-1}\bar{B}K_r^{-1})\ddot{q}_m + F_m\dot{q}_m + \tau_{NL} \tag{5}$$

where

$$\tau_{NL} = K_r^{-1}\Delta B K_r^{-1}\ddot{q}_m + K_r^{-1}C K_r^{-1}\dot{q}_m + K_r^{-1}g. \tag{6}$$

As evidenced by the block diagram scheme of Fig. 1, the system of the manipulator structure and the mechanical part of the gear reductions is actually composed of two subsystems; one with τ_m as input and q_m as output, the other with q_m, $\dot{q}_m$, $\ddot{q}_m$ as input and τ_{NL} as output. The former is *linear* and *decoupled*; each component of τ_m affects the corresponding component of q_m. The latter is *nonlinear* and *coupled*, since it accounts for all those nonlinear and interacting contributions stemming from the joint coupled dynamics.

On the basis of the above scheme, τ_{NL} can be regarded as a vector of *disturbance* forces for the joint servos. This corresponds to a *decentralized* structure of the controller, since each joint is controlled independenty from the others.

3. Disturbance Rejection

It is desired to find a control structure that allows satisfactory tracking of the output reference variable with suitable reduction of disturbance effects; hence, the two goals of the design are *disturbance rejection* and *trajectory tracking*. Let then face up to the problem of disturbance rejection, first.

The system to control is the servo of the ith joint of the manipulator. This presents the block diagram scheme of Fig. 2, which is logically derived from the scheme in Fig. 1. In detail, the ith motor is characterized by the average inertia

$$I_{Ti} = I_{mi} + k_{ri}^{-2}\bar{b}_{ii},$$

the resistance of the armature circuit R_{ai} (the inductance has been neglected), and the torque and voltage constants k_{ti} and k_{vi}, respectively. Further, G_{vi} indicates the voltage gain of the power amplifier that usually preceeds the motor. Consequently, the input to the system is not the armature voltage v_{ai}, but the input voltage v_{ci} of the amplifier. The scheme of Fig. 2 evidences the presence of the disturbance input d_i that turns out to be the ith component of the torque vector τ_{NL} in (6), i.e.

$$d_i = \sum_{k=1}^{n} k_{ri}^{-1} k_{rk}^{-1} b_{ik} \ddot{\theta}_k - k_{ri}^{-2} \bar{b}_{ii} \ddot{\theta}_i + \sum_{k=1}^{n} k_{ri}^{-1} k_{rk}^{-1} c_{ik} \dot{\theta}_k + k_{ri}^{-1} g_i \tag{7}$$

where $\bar{b}_{ii}$ is the average, constant value of inertia at the ith joint, and k_{ri} is the gear ratio of the ith joint. Notice that in the scheme of Fig 2, the viscous friction coefficient F_{mi} has been assumed negligible with respect to the equivalent electrical friction coefficient $k_{vi} k_{ti}/R_{ai}$. Moreover, the following positions are made:

$$k_{mi} = \frac{1}{k_{vi}} \qquad \tau_{mi} = \frac{R_{ai} I_{Ti}}{k_{vi} k_{ti}}$$

where k_{mi} and τ_{mi} are respectively the gain and time constants of the motor; G_{vi} is considered to be included in the controller gain. Hence, the motor is described by the voltage to position transfer function —dropping, from now on, the subscript i for notation compactness—

$$G(s) = \frac{k_m}{s(1 + sT_m)}. \tag{8}$$

An effective rejection of the disturbance d is ensured by:

- a large value of the power amplifier gain,
- an integral action in the controller so that the effect of the gravitational component on the output θ is annihilated at steady-state.

This clearly suggests the use of a *PI* action for the controller whose transfer function is

$$C(s) = K_c \frac{1 + sT_c}{s};$$

this yields zero error at steady-state for a step disturbance, and the presence of the real zero in $s = -1/T_c$ offers a stabilizing function.

Besides the closure of a position feedback loop, the most general solution is obtained by closing inner feedback loops on the velocity and acceleration. This leads to the scheme in Fig. 3, where $C_P(s)$, $C_V(s)$, $C_A(s)$ represent respectively the *position, velocity, acceleration* controllers, k_{TP}, k_{TV}, k_{TA} are the relative transducer costants, and the amplifier gain constant has been embedded in the gain constant of the inmost controller. Notice also that the disturbance torque d has been appropriately transformed into a disturbance voltage by the factor R_a/k_t.

In the following, the three particular solution that derive from the general scheme of Fig. 3 are presented; at this stage, the eventual issue arising from measurement of physical variables is not considered yet.
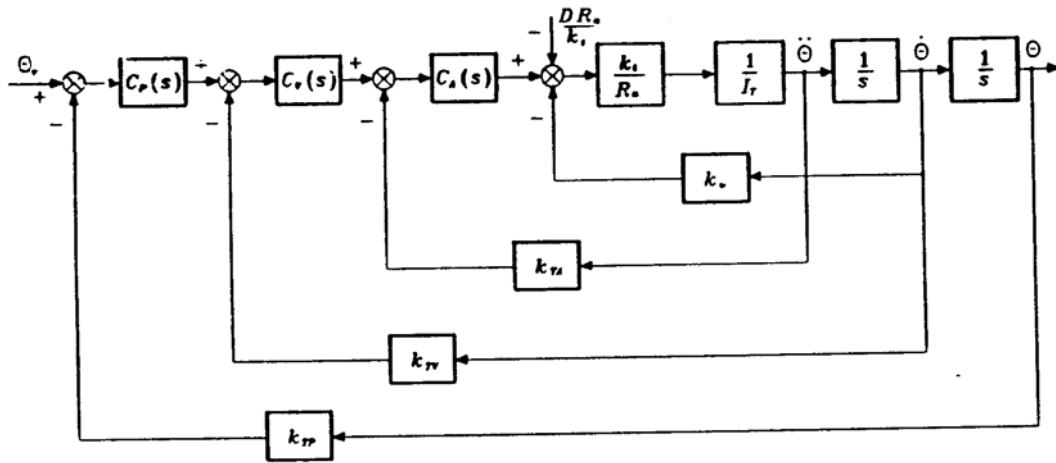
Figure 3 — Block diagram scheme of the position + velocity + acceleration feedback control system.

3.1 Position Feedback

In this case:

$$C_P(s) = K_P\frac{1 + sT_P}{s}, \; C_V(s) = 1, \; C_A(s) = 1$$

$$k_{TV} = k_{TA} = 0.$$

Root locus analysis can be performed as the gain of the position loop varies. Three situations are evidenced for the closed-loop poles (Fig. 4). The stability of the closed-loop feedback system imposes some constraints on the choice of the parameters of the PI regulator: If $T_P < T_m$, the system is inherently unstable (Fig. 4a). Then, it must be $T_P > T_m$ (Fig. 4b). As T_P increases, however, the absolute value of the real part of the two roots of the locus tending towards the asymptotes increases too, and the system has faster time response. Hence, it is convenient to render $T_P \gg T_m$ (Fig. 4c). In any case, the real part of the couples of dominant poles cannot be less than $-T_m/2$.

The closed-loop input/output transfer function is

$$\frac{\Theta(s)}{\Theta_i(s)} = \frac{\frac{1}{k_{TP}}}{1 + \frac{s^2(1 + sT_m)}{k_m K_P k_{TP}(1 + sT_P)}}, \tag{9}$$

while the closed-loop disturbance/output transfer function is

$$\frac{\Theta(s)}{D(s)} = -\frac{\frac{sR_a}{k_t K_P k_{TP}(1 + sT_P)}}{1 + \frac{s^2(1 + sT_m)}{k_m K_P k_{TP}(1 + sT_P)}}. \tag{10}$$

$$T_P < T_m \qquad \frac{k_m K_P k_{TP} T_P}{T_m}$$

a)

$$-\frac{1}{T_P} \quad -\frac{1}{T_m} \qquad (2)$$

$$T_P > T_m \qquad \frac{k_m K_P k_{TP} T_P}{T_m}$$

b)

$$-\frac{1}{T_m} \quad -\frac{1}{T_P} \qquad (2)$$

$$T_P \gg T_m \qquad \frac{k_m K_P k_{TP} T_P}{T_m}$$

c)

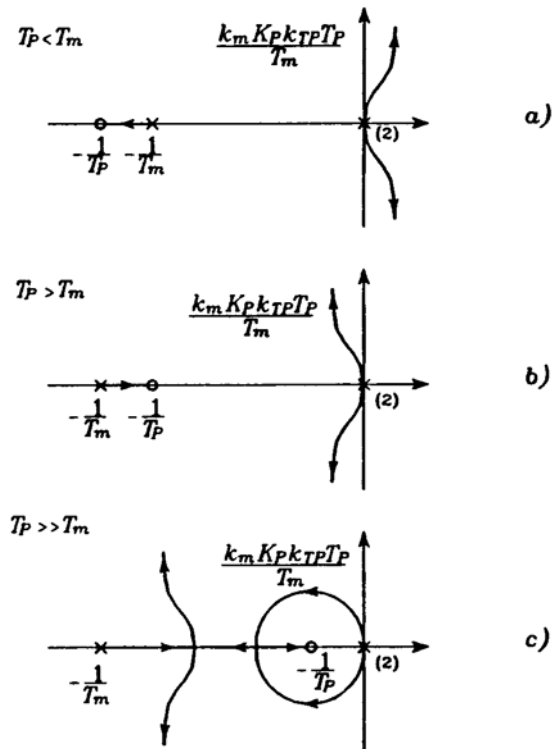$$-\frac{1}{T_m} \qquad -\frac{1}{T_P} \quad (2)$$

Figure 4 — Root loci for the position feedback scheme.

It can be recognized that the term $K_P k_{TP}$ is the reduction factor imposed by the feedback gain on the amplitude of the output due to the disturbance; then, the quantity

$$X_R = K_P k_{TP} \tag{11}$$

can be interpreted as the disturbance rejection factor. However, it is not appropriate to increase K_P too much, because small damping ratios would result leading to unacceptable oscillations of the output. Further, for large values of K_P, the third root on the real axis is almost canceled by the neighboring zero. On the other hand, it can be noticed in (10) that also the closed-loop zero in $s = -1/T_P$ is canceled by the pole at denominator; thus, the closed-loop pole close to the zero is not canceled anymore and then determines the dynamics of the disturbance, which is quite slow. A characterization of the recovery time to the disturbance is then given by the time constant
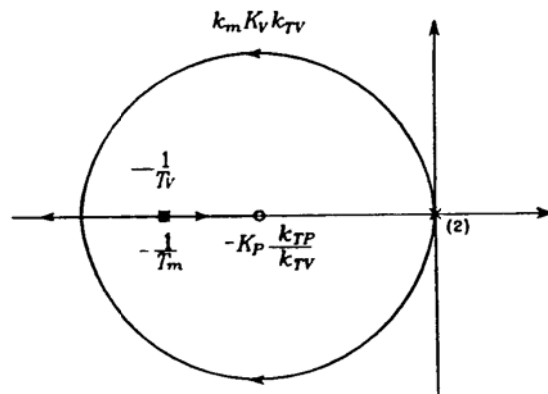
$$T_R = T_P. \tag{12}$$

Figure 5 — Root locus for the position + velocity feedback scheme.

3.2 Position + Velocity Feedback

In this case:

$$C_P(s) = K_P, \ C_V(s) = K_V \frac{1 + sT_V}{s}, \ C_A(s) = 1$$

$$k_{TA} = 0.$$

Root locus analysis can be performed as the gain of the velocity loop varies. The most convenient choice is to utilize the zero of the regulator in $s = -1/T_V$ to cancel the effects of the real pole of the motor in $s = -1/T_m$. By setting

$$T_V = T_m,$$

the poles of the closed-loop system move on the root locus as the gain of the velocity loop varies (see Fig. 5). The increase of K_P allows to move the roots towards regions of the left-half complex plane characterized by large values of the real part, if an opportune choice of K_V is made.

The closed-loop input/output transfer function is

$$\frac{\Theta(s)}{\Theta_i(s)} = \frac{\frac{1}{k_{TP}}}{1 + \frac{sk_{TV}}{K_P k_{TP}} + \frac{s^2}{k_m K_P k_{TP} K_V}}, \tag{13}$$

which can be compared with the typical transfer function of a second-order system

$$W(s) = \frac{\frac{1}{k_{TP}}}{1 + \frac{2\zeta s}{\omega_n} + \frac{s^2}{\omega_n^2}}. \tag{14}$$

It can be recognized that, with a suitable choice of the gains, it is possible to get all the values of natural frequency ω_n and damping ratio ζ. Hence, if ω_n and ζ are given as design requirements, the following relations can be established:

$$K_V k_{TV} = \frac{2\zeta\omega_n}{k_m} \tag{15}$$

$$K_P k_{TP} K_V = \frac{\omega_n^2}{k_m}. \tag{16}$$

Once K_V and k_{TV} have been chosen to satisfy (15), the values of K_P and k_{TP} are obtained from (16).

Further, the closed-loop disturbance/output transfer function is

$$\frac{\Theta(s)}{D(s)} = -\frac{\frac{sR_a}{k_t K_P k_{TP} K_V(1 + sT_V)}}{1 + \frac{sk_{TV}}{K_P k_{TP}} + \frac{s^2}{k_m K_P k_{TP} K_V}}, \tag{17}$$

which shows that the disturbance rejection factor is

$$X_R = K_P k_{TP} K_V \tag{18}$$

and is fixed, once K_P and K_V have been chosen via (15,16). Concerning the disturbance dynamics, the presence of a zero in the origin introduced by the PI and of three poles having real parts $-1/T_V$, $-\zeta\omega_n$, $-\zeta\omega_n$ should be noticed. Hence, in this case, an estimate of the disturbance recovery time is given by the time constant

$$T_R = \sup\{T_m, \frac{1}{\zeta\omega_n}\}, \tag{19}$$

which reveals an improvement with respect to the previous case in (11), since $T_m \ll T_P$.

3.3 Position + Velocity + Acceleration Feedback

In this case:

$$C_P(s) = K_P, C_V(s) = K_V, C_A(s) = K_A \frac{1 + sT_A}{s}.$$

Differently form the previous case, the presence of the acceleration feedback does not allow to define the motor transfer function as in (8). It is necessary, in fact, to perform some handy manipulation of the block diagram scheme in Fig. 3, so as to report the acceleration loop in parallel to the velocity loop of the motor. It can be shown that, also in this case, an opportune cancellation can be performed by setting
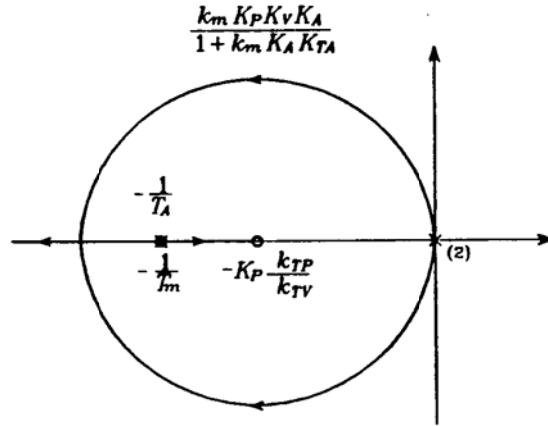
$$T_A = T_m$$

$$\frac{k_m K_P K_V K_A}{1 + k_m K_A K_{TA}}$$

Figure 6 — Root locus for the position + velocity + acceleration feedback scheme.

or

$$k_m K_A k_{TA} T_A \gg T_m \qquad k_m K_A k_{TA} \gg 1.$$

The two solutions are essentially the same, as far as the dynamic features of the control system are concerned. In both cases, in fact, the closed-loop poles are constrained on the root locus in Fig. 6. This turns out to be analogous to the one in Fig. 5, having assimilated the system to a second-order one.

The closed-loop input/output transfer function is

$$\frac{\Theta(s)}{\Theta_i(s)} = \frac{\frac{1}{k_{TP}}}{1 + \frac{s k_{TV}}{K_P k_{TP}} + \frac{s^2(1 + k_m K_A k_{TA})}{k_m K_P k_{TP} K_V K_A}}. \tag{20}$$

Moreover, the closed-loop disturbance/output transfer function is

$$\frac{\Theta(s)}{D(s)} = -\frac{\frac{s R_a}{k_t K_P k_{TP} K_V K_A(1 + s T_A)}}{1 + \frac{s k_{TV}}{K_P k_{TP}} + \frac{s^2(1 + k_m K_A k_{TA})}{k_m K_P k_{TP} K_V K_A}}. \tag{21}$$

The resulting disturbance rejection factor and recovery time are respectively given by

$$X_R = K_P k_{TP} K_V K_A \tag{22}$$

and

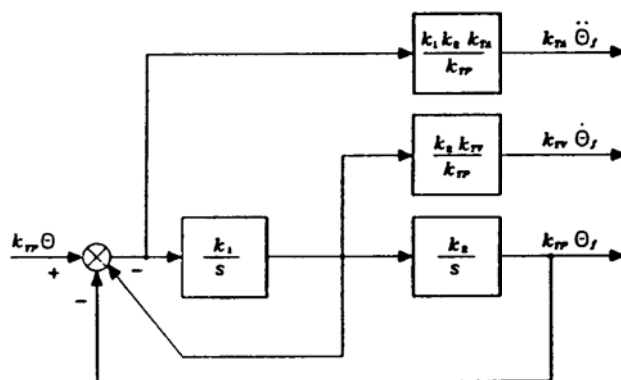$$T_R = \sup\{T_A, \frac{1}{\zeta \omega_n}\} \tag{23}$$

Figure 7 — Block diagram scheme of the state variable filter.

where T_A can be made less than T_m.

With reference to the transfer function in (14), the following relations can be established for design purposes:

$$\frac{2K_P k_{TP}}{k_{TV}} = \frac{\omega_n}{\zeta} \tag{24}$$

$$1 + k_m K_A k_{TA} = \frac{k_m X_R}{\omega_n^2} \tag{25}$$

$$K_P k_{TP} K_V K_A = X_R. \tag{26}$$

Once K_P, k_{TP} and k_{TV} have been chosen to satisfy (24), K_A and k_{TA} are chosen to satisfy (25), and then K_V is obtained from (26). Therefore, with respect to the previous case, now the acceleration feedback remarkably allows not only to achieve any desired dynamic behavior, but also to prescribe the disturbance rejection factor.

In deriving the above three control schemes, the issue of measurement of feedback variables was not considered explicitly. With reference to the typical position control servos that are implemented in industrial practice, there is no problem to measure position and velocity, while a direct measurement of acceleration in general either is not available or is too expensive to get. Therefore, for the general scheme of Fig. 3 with position + velocity + acceleration feedback, an indirect measure is to be obtained, that is the acceleration measurement is reconstructed from the position measurement by means of a state variable filter (Fig. 7). The filter is characterized by a natural frequency $\omega_{nf} = \sqrt{k_1 k_2}$ and by a damping ratio $\zeta_f = (1/2)\sqrt{k_1/k_2}$. Choosing the filter bandwidth to be larger than the joint servo bandwidth —at least a decade off to the right— the effects due to measurement lags between θ_f and θ are not appreciable, and then it is feasible to take the filter outputs as the quantities to feed back.

4. Trajectory Tracking

The above schemes have been derived according to the purpose of achieving good disturbance rejection. When the joint control servos are required to track reference position trajectories with high values of speed and acceleration, the tracking capabilities of the scheme in Fig. 3 may become quite poor.

A computationally cheap remedy to the above inconvenient can be obtained via the well-known technique of feedforward cancellation of the plant dynamics. In particular, it is quite straightforward to recognize that if the reference inputs to the three control structures analyzed in the previous section are modified respectively into

$$\Theta_i = \left(k_{TP} + \frac{s^2(1 + sT_m)}{k_m K_P(1 + sT_P)} \right) \Theta_d \qquad (27)$$

$$\Theta_i = \left(k_{TP} + \frac{s k_{TV}}{K_P} + \frac{s^2}{k_m K_P K_V} \right) \Theta_d \qquad (28)$$

$$\Theta_i = \left(k_{TP} + \frac{s k_{TV}}{K_P} + \frac{(1 + k_m K_A k_{TA})s^2}{k_m K_P K_V K_A} \right) \Theta_d, \qquad (29)$$

perfect tracking of the desired joint position trajectory is achieved. Incidentally, computing derivatives of the desired trajectory $\theta_d(t)$ is not a problem, once that is known analytically.

All the solutions allow perfect tracking of the input trajectory within the range of validity and linearity of the employed models. Deviations from the ideal values cause a performance degradation that must be analyzed case by case. It is interesting to notice that, as the number of nested feedback loops increases, less knowledge of the system model is required to perform feedforward compensation. In fact, T_m and k_m are required to close a position loop, only k_m is required for the position + velocity loops, and k_m again —but with reduced weight— for the position + velocity + acceleration loops.

Finally, we remark that the disturbance is not completely unknown but an expression is given in (7), though it is only an approximate one. Therefore, it is understood that a model-based compensation can be performed —say in a feedforward fashion, so as to perform it off-line for typically repetitive trajectories— which can alleviate the endeavor of disturbance rejection of the previous schemes. In other words, a valid solution from an engineering viewpoint could be that of devising the control system for an industrial robot manipulator as composed of two subsystems; a decentralized robust independent joint control with acceleration feedback whose performance can be enhanced by the introduction of a centralized model-based (feedforward) control that compensates for the relevant contributions of manipulator dynamics.

5. Conclusions

The design of independent joint controllers for industrial robot manipulators has been investigated in this work as a still valid alternative to model-based control algorithms. Three schemes have been developed using classical linear control techniques. In particular, one scheme that adopts position + velocity + acceleration feedback, with the help of a state variable filter to reconstruct acceleration measurements, has been shown to guarantee excellent disturbance rejection performance. Preliminary simulation results for a three-joint industrial manipulator are reported in [9]. A future paper will describe experimental tests which we are currently conducting on a high-speed parallel robot.

References

[1] P.K. Khosla and T. Kanade, "Experimental evaluation of nonlinear feedback and feedforward control schemes for manipulators," *Int. J. of Robotics Research*, vol. 7, no. 1, pp. 18–28, 1988.

[2] J.J. Craig, *Introduction to Robotics: Mechanics and Control*, 2nd Ed., Addison Wesley, Reading, MA, 1989.

[3] M.W. Spong and M. Vidyasagar, *Robot Dynamics and Control*, John Wiley & Sons, New York, 1989.

[4] A. Balestrino, G. De Maria, and L. Sciavicco, "An adaptive model following control for robotic manipulators," *ASME J. of Dynamic Systems, Measurements, and Control*, vol. 105, pp. 143–151, 1983.

[5] J.-J.E. Slotine and W. Li, "On the adaptive control of robot manipulators," *Int. J. of Robotics Research*, vol. 6, no. 3, pp. 49–59, 1987.

[6] R. Ortega and M.W. Spong, "Adaptive motion control of rigid robots: A tutorial," *Automatica*, vol. 25, pp. 877-888, 1989.

[7] M.B. Leahy Jr. and G.N. Saridis, "Compensation of industrial manipulator dynamics," *Int. J. of Robotics Research*, vol. 8, no. 4, pp. 73–84, 1989.

[8] P. Chiacchio, L. Sciavicco, and B. Siciliano, "The potential of model-based control algorithms for improving industrial robot tracking performance," *Proc. IEEE Int. Workshop on Intelligent Motion Control*, Istanbul, TR, pp. 831–836, 1990.

[9] P. Chiacchio, L. Sciavicco, and B. Siciliano, "Practical design of independent joint controllers for industrial robot manipulators," *1992 American Control Conf.*, Chicago, IL, June 1992.